

# Word4Per: Zero-shot Composed Person Retrieval

Delong Liu  
liudelong@bupt.edu.cn  
Beijing University of Posts and  
Telecommunications  
Beijing, China

Haiwen Li  
lihaiwen52@bupt.edu.cn  
Beijing University of Posts and  
Telecommunications  
Beijing, China

Zhicheng Zhao\*  
zhaozc@bupt.edu.cn  
Beijing University of Posts and  
Telecommunications  
Beijing Key Laboratory of Network  
System and Network Culture  
Beijing, China

Fei Su  
sufei@bupt.edu.cn  
Beijing University of Posts and  
Telecommunications  
Beijing Key Laboratory of Network  
System and Network Culture  
Beijing, China

Yuan Dong  
yuandong@bupt.edu.cn  
Beijing University of Posts and  
Telecommunications  
Beijing Key Laboratory of Network  
System and Network Culture  
Beijing, China

## ABSTRACT

Searching for specific person has great social benefits and security value, and it often involves a combination of visual and textual information. Conventional person retrieval methods, whether image-based or text-based, usually fall short in effectively harnessing both types of information, leading to the loss of accuracy. In this paper, a whole new task called Composed Person Retrieval (CPR) is proposed to jointly utilize both image and text information for target person retrieval. However, the supervised CPR requires very costly manual annotation dataset, while there are currently no available resources. To mitigate this issue, we firstly introduce the Zero-shot Composed Person Retrieval (ZS-CPR), which leverages existing domain-related data to resolve the CPR problem without expensive annotations. Secondly, to learn ZS-CPR model, we propose a two-stage learning framework, Word4Per, where a light-weight Textual Inversion Network (TINet) and a text-based person retrieval model based on fine-tuned Contrastive Language-Image Pre-training (CLIP) network are learned without utilizing any CPR data. Thirdly, a finely annotated Image-Text Composed Person Retrieval (ITCPR) dataset is built as the benchmark to assess the performance of the proposed Word4Per framework. Extensive experiments under both Rank-1 and mAP demonstrate the effectiveness of Word4Per for the ZS-CPR task, surpassing the comparative methods by over 10%. The code and ITCPR dataset will be publicly available at <https://github.com/Delong-liu-bupt/Word4Per>.

## KEYWORDS

Zero-shot, Composed Person Retrieval, ITCPR Dataset, Textual Inversion Network

## 1 INTRODUCTION

Person retrieval [20, 50] aims to identify target person images from a large-scale person gallery. It comprises two popular directions: Image-based Person Retrieval (IPR) [32] and Text-based Person Retrieval (TPR) [25], which are dedicated to using images

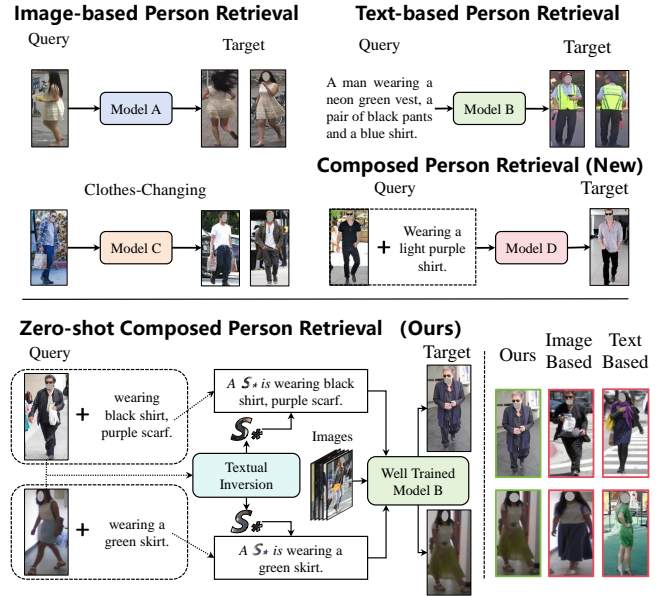


**Figure 1: Existing methods and our proposed new task. Top: IPR aims to train a model (Model A and Model C) to identify the target person using a reference image, while TPR models (Model B) find the target person using text. Our proposed CPR task aims to learn a model (Model D) to identify the target by combining visual and textual information. Bottom: To avoid using of costly triplets data to train Model D, we introduce the ZS-CPR task and propose a solution: Word4Per.**

and texts commonly acquired in daily life as queries to identify the targets of interest. In recent years, due to its extensive applications in social services and public security, person retrieval has garnered increasing attention.

In real scenarios, when seeking a specific person, both visual and textual information are often available, while IPR and TPR methods

\*Corresponding author

can not fully leverage all information, inevitably leading to a certain loss in accuracy. Therefore, as shown in Figure 1, we propose a novel task, Composed Person Retrieval (CPR), to simultaneously utilize visual and textual information for retrieving the target person. The CPR task is a variant of the Composed Image Retrieval (CIR) task [1], where the dataset consists of a large number of triplets  $(I_q, T_q, I_t)$ , comprising a reference image  $(I_q)$ , a relative caption  $(T_q)$ , and several target images  $(I_t)$ . This type of data is manually collected and annotated and this process is time-consuming and expensive. Moreover, previous research [4, 17] in the CIR field has shown that training a fully supervised network (*Model D*) heavily depends on large-scale dataset, which is not available for the CPR task.

To address this challenge, we introduce a new task named as Zero-shot Composed Person Retrieval (ZS-CPR), aiming to present a new method that no longer relies on costly triplet annotations for supervised learning but rather uses existing image-caption data to solve the CPR issue. And correspondingly, a two-stage framework called Word4Per is proposed to learn the ZS-CPR model, where image-caption datasets [8, 25, 57] for the TPR task are utilized. Specifically, in the first stage, we introduce a cross-modal retrieval network to maximize the similarity between person images and their captions. In the second stage, a lightweight Textual Inversion Network (TINet) is constructed to map the image into a special word. By this way, a flexible combination of reference image and relative caption for retrieval can be obtained. Furthermore, for effective evaluation the performance of Word4Per method, a test set ITCPR is constructed via reusing public person retrieval datasets such as Celeb-reID [18], LAST [40], and PRCC [49]. Annotating the relative captions is achieved by selecting images of the same identity with different outfits, and finally, a complete set of triplets is created.

As shown in Figure 1, in practical applications, the trained TINet is used to transform the reference image  $I_q$  into a pseudo-word  $S_*$ . Subsequently, this pseudo-word is concatenated via using a sentence template with the relative caption  $T_q$ . The well-trained *Model B* is then used for person retrieval, finding the corresponding targets.

To validate the effectiveness of our proposed the Word4Per framework and ITCPR dataset for the ZS-CPR task, extensive experiments are conducted. The experimental results show significant improvements in evaluation metrics compared to the state-of-the-art methods [20, 37]. The main contributions can be summarized as follows:

- A novel cross-modal task, named zero-shot composed person retrieval, is proposed to deal with the CPR problem without costly triplet annotations.
- We propose an efficient and flexible Word4Per framework for ZS-CPR, in which a lightweight textual inversion network and a TPR model are learned without utilizing any CPR triplets data.
- We annotate and build a new ITCPR dataset for the ZS-CPR task.
- Extensive experiments validate the effectiveness of our proposed Word4Per framework and ITCPR dataset.

## 2 RELATED WORK

### 2.1 Person Retrieval

Person retrieval consists of two main branches: IPR and TPR. IPR, the older subfield, has witnessed extensive research on feature extraction [32, 33, 41], metric learning [15], lightweight models [23, 36, 56], multi-branch methods [43, 50], and attention mechanisms [3, 52]. Recently, transformer-based models like PAT [28], DRL-Net [19], and TransReID [14] have gained popularity by combining ResNet-50 [13] with Transformer [42] decoders, achieving outstanding performance on large datasets. A recent popular variant of the IPR task is clothes-changing person retrieval [18], aimed at finding the same person with different clothing. This field has given rise to a plethora of datasets [18, 40, 49] and works [34, 48].

In contrast, TPR [25] is a relatively younger field, but it has progressed rapidly thanks to the development of text-image pre-training models [24, 37]. TPR aims to align image and text features in a shared embedding space to facilitate person matching. Early TPR methods [5, 55] primarily focused on extracting global [55] and local features [5, 51] from image-text pairs and then using matching loss for modality alignment. However they often struggled to balance efficiency and performance. Recent research [20, 29, 46] has introduced auxiliary tasks, to enable implicit feature alignment, thereby enhancing performance without increasing inference complexity. In [20], the pre-trained language-image model (CLIP) [37] was directly applied to TPR. However, the existing methods still do not effectively fused text and image information to find the target person, despite it is a common application.

### 2.2 Composed Image Retrieval

Composed Image Retrieval (CIR) [4, 17, 22] aims to achieve diverse image retrieval by merging image and text queries. This task belongs to the broader field of compositional learning [1, 6] and has been explored in various domains like fashion [12, 45] and scene composition [30], booming different fusion and training techniques. For instance, self-training shallow Transformers [42] and pre-trained Bert [7] models were utilized to fuse images and texts. However, these methods typically required training on carefully annotated CIR datasets [30, 45] and only performed effectively on images related to the training set. Consequently, the Zero-Shot Composed Image Retrieval (ZS-CIR) [2, 38] has been introduced. They leveraged the powerful modality alignment capabilities of big models like CLIP to convert image information into pseudo-text information [9], enabling the completion of the task without CIR dataset. Though the CPR task can be considered as a subtask of CIR, the existing methods are not suitable for CPR.

## 3 METHOD

The proposed Word4Per framework is shown in Figure 2, and it consists of two main parts: fine-tuning the CLIP network and learning a TINet. Firstly, to align visual-textual features well, we fine-tune the CLIP network by introducing three supervised losses. Subsequently, a lightweight TINet is proposed to optimize the transformation of visual information into pseudo-word, where the visual and text encoders are frozen, and contrastive learning losses are employed. During the inference, the trained TINet is firstly used

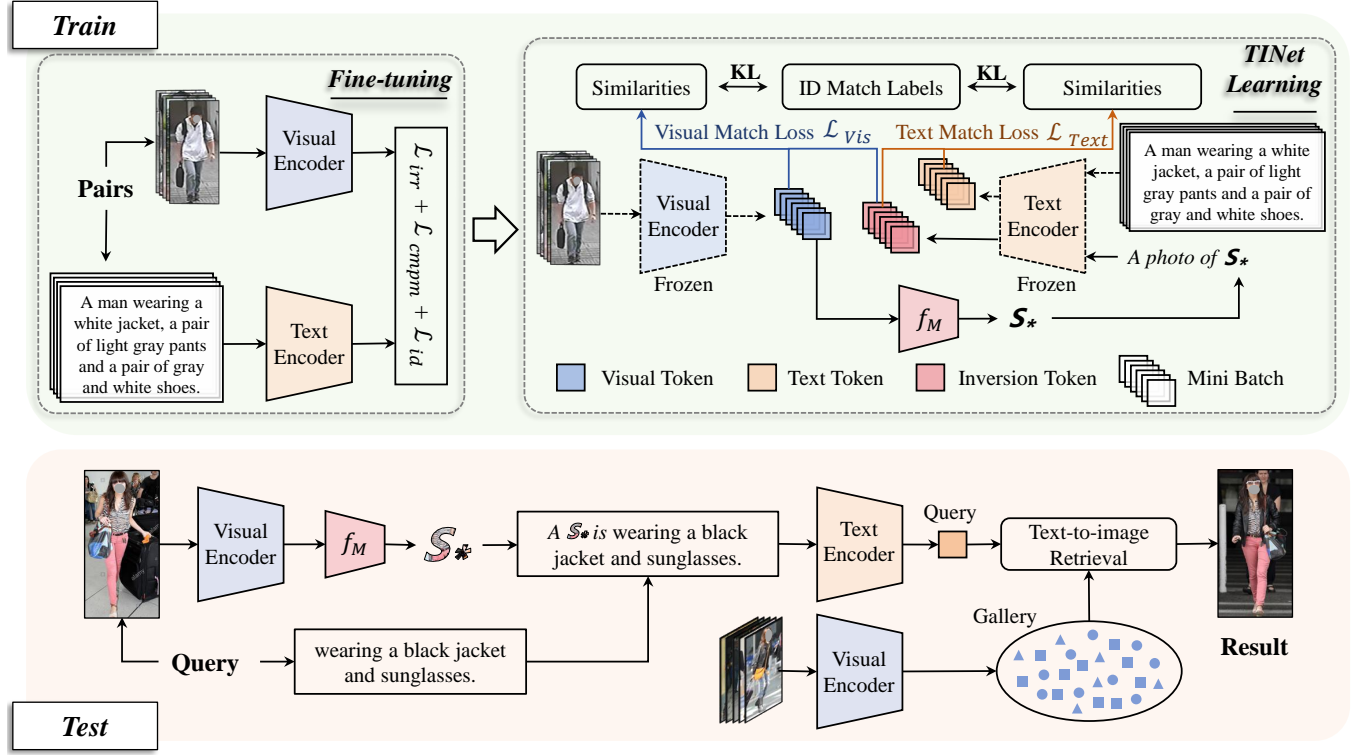


**Figure 2: Training and inference of the Word4Per framework. Top: The training process is divided into two stages, and the first one is the fine-tuning phase, in which three losses ( $\mathcal{L}_{irr}$ ,  $\mathcal{L}_{cmpm}$ ,  $\mathcal{L}_{id}$ ) are used to optimize the visual and text encoders. The second stage is the training of the TINet  $f_M$ , where two contrastive learning losses  $\mathcal{L}_{Vis}$  and  $\mathcal{L}_{Text}$  are applied to supervise the generation of pseudo-word  $S_*$ . Bottom: During the testing phase, the well-trained dual encoders and TINet are used to accomplish CPR task.**

to generate pseudo-word token, which is then inserted into a sentence template along with the relative caption and fed into the text encoder, to produce the final text features for person retrieval.

### 3.1 Fine-tuning of CLIP Network

Considering that pre-training data of CLIP is comprehensive and not specifically tailored for person retrieval, thus we fine-tune it based on image-caption data of person retrieval. In our implementation, we adopt an effective feature alignment network [20] to achieve this.

The fine-tuning primarily solves identity issues of image-text pairs that are not covered in the pre-training, as well as finer details in person descriptions. To do this, different losses are introduced to supervise features from different modalities, while aggregating different modality representations of the same identity, and emphasizing the fine-grained textual descriptions corresponding to images.

The whole fine-tuning of our Word4Per involves three kinds of supervisions. Specifically, to discover finer relationships between image and text, an implicit relation reasoning loss  $\mathcal{L}_{irr}$  [20] is introduced.  $\mathcal{L}_{irr}$  is calculated by contrasting the probability distribution of words predicted using visual information with the actual

distribution, and it is computed as follows:

$$\mathcal{L}_{irr} = -\frac{1}{|\mathcal{M}| \cdot |\mathcal{V}|} \sum_{i \in \mathcal{M}} \sum_{j \in |\mathcal{V}|} y_j^i \log \frac{\exp(m_j^i)}{\sum_{k=1}^{|\mathcal{V}|} \exp(m_k^i)}, \quad (1)$$

where  $\mathcal{M}$  represents a set of masked text tokens,  $|\mathcal{V}|$  represents the vocabulary size,  $y_j^i$  is a one-hot vocabulary distribution where the ground-truth token has a probability of 1, and  $m_j^i$  is the predicted word distribution probability.

Moreover, aiming to match feature representations between different modalities, inspired by [51], a cross-modal projection matching loss  $\mathcal{L}_{cmpm}$  is adopted.  $\mathcal{L}_{cmpm}$  utilizes cosine similarity distributions to compute matching probabilities for  $N \times N$  image-text pairs within a mini batch and employs KL divergence to measure the difference between these probabilities and the true matching labels. For each global embedding  $f_i^v$  of an image, we can create a set of image-text embedding pairs  $\left\{ \left( f_i^v, f_j^t \right), l_{i,j} \right\}_{j=1}^N$ , where  $l_{i,j}$  is the true matching label.  $l_{i,j} = 1$  indicates that  $\left( f_i^v, f_j^t \right)$  forms a matching pair from the same identity, while  $l_{i,j} = 0$  denotes a non-matching pair. The cosine similarity between  $\mathbf{u}$  and  $\mathbf{v}$ ,  $\text{sim}(\mathbf{u}, \mathbf{v}) = \mathbf{u}^T \mathbf{v} / \|\mathbf{u}\| \|\mathbf{v}\|$ , is

$\mathcal{L}_2$  normalized. The formula for calculating the matching probability is as follows:

$$p_{i,j} = \frac{\exp\left(\text{sim}\left(f_i^v, f_j^t\right) / \tau\right)}{\sum_{h=1}^N \exp\left(\text{sim}\left(f_i^v, f_h^t\right) / \tau\right)}, \quad (2)$$

where  $\tau$  is a temperature hyperparameter controlling the peak of the probability distribution. Within a mini batch, the image-to-text matching loss is calculated using the following formula:

$$\mathcal{L}_{i2t} = KL(p_i \| q_i) = \frac{1}{N} \sum_{i=1}^N \sum_{j=1}^N p_{i,j} \log\left(\frac{p_{i,j}}{q_{i,j} + \epsilon}\right), \quad (3)$$

where  $\epsilon$  is a small value to avoid numerical issues, and  $q_{i,j} = l_{i,j} / \sum_{k=1}^N l_{i,k}$  represents the true matching probability.

Similarly, the text-to-image matching loss  $\mathcal{L}_{t2i}$  can be formalized by swapping  $f^v$  and  $f^t$  in equations (2) and (3), and the bidirectional matching loss  $\mathcal{L}_{cmpm}$  is calculated as follows:

$$\mathcal{L}_{cmpm} = \mathcal{L}_{i2t} + \mathcal{L}_{t2i}. \quad (4)$$

Furthermore, a common ID loss ( $\mathcal{L}_{id}$ ) [55] is used to supervise identity label. Therefore, the overall optimization objective for the fine-tuning is:

$$\mathcal{L} = \mathcal{L}_{irr} + \mathcal{L}_{cmpm} + \mathcal{L}_{id}. \quad (5)$$

### 3.2 Learning the Textual Inversion Network

As mentioned before, the TINet is designed to achieve the mapping from image information to the linguistic space, where both image and word information in CLIP are represented by one-dimensional fixed-length vectors. Therefore, the TINet offers highly lightweight choice, allowing the mapping to be completed with minimal optimization complexity and optimal implementation speed. Specifically, in this paper, we opt for a shallow fully connected network. Based on image-text pairs, the TINet is learnt to map the global representation  $f_i^v$  of an image into pseudo-word token. Considering that the images and texts for the same identity are highly related, the loss function for TINet optimization needs to include the identity information.

As shown in the top of Figure 2, after completing the fine-tuning of the dual encoders, the training of the TINet is conducted with the dual encoders fully frozen. For the same batch of  $N$  image-text pairs, it is still able to construct a set of image-text representation pairs  $\{(f_i^v, f_j^t), l_{i,j}\}_{j=1}^N$ , where  $l_{i,j}$  represents the real matching labels. The global embedding  $f_i^v$  of each image is used to obtain pseudo-word embeddings as tokens  $S_* = f_M(f_i^v)$ . Subsequently, it is appended to the end of token embeddings of the prompt sentence, "a photo of", resulting in  $\hat{S}_*$ . Then  $\hat{S}_*$  is fed into the text encoder to obtain textual inversion embedding  $f_k^c, k = 1, 2, \dots, N$ . Similarly, we obtain the set of embeddings for image and textual inversion pairs  $\{(f_i^v, f_k^c), l_{i,k}\}_{k=1}^N$  and the corresponding set of text and textual inversion encoding pairs  $\{(f_j^t, f_k^c), l_{j,k}\}_{k=1}^N$ , where the real matching labels  $l_{i,k}$  and  $l_{j,k}$  are equal to the corresponding positions of  $l_{i,j}$ .

Through TINet, each pseudo-word embedding is expected to closely match the corresponding image. Therefore, the contrastive

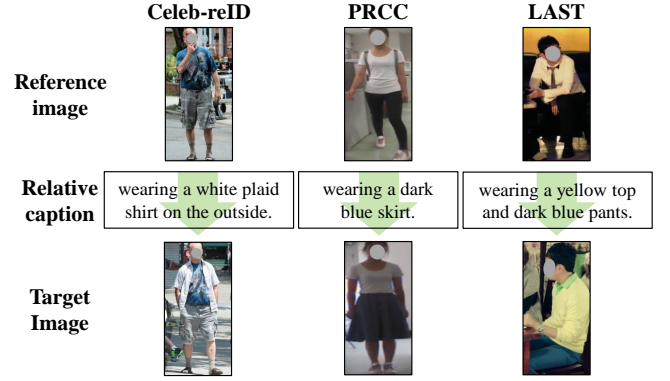


Figure 3: Examples of queries and ground truths in our ITCPR dataset.

learning loss based on  $\mathcal{L}_{cmpm}$  is introduced to achieve this objective, i.e.,

$$\begin{cases} \mathcal{L}_{Vis} = \mathcal{L}_{i2c} + \mathcal{L}_{c2i}, \\ \mathcal{L}_{Text} = \mathcal{L}_{t2c} + \mathcal{L}_{c2t}, \end{cases} \quad (6)$$

where  $\mathcal{L}_{i2c}$  is computed by replacing  $f^t$  with  $f^c$  in equations (2) and (3),  $\mathcal{L}_{c2i}$  is computed by replacing  $f^v$  with  $f^c$  and  $f^t$  with  $f^v$ ,  $\mathcal{L}_{t2c}$  is computed by replacing  $f^v$  with  $f^t$  and  $f^t$  with  $f^c$ , and  $\mathcal{L}_{c2t}$  is computed by replacing  $f^v$  with  $f^c$ . The  $\mathcal{L}_{Vis}$  focuses more on visual information in the image, while the  $\mathcal{L}_{Text}$  focuses more on semantic information corresponding to the image.

Fine-tuning of CLIP and training of TINet are crucial for the Word4Per to acquire the combined zero-shot retrieval capability. TINet's training relies on a highly aligned dual encoder, and the trained TINet can convert image information into pseudo-word that can be easily concatenated to sentences, thereby transforming the CPR task into a general TPR task implemented by fine-tuned CLIP.

### 3.3 Inference

During inference, a reference image with a relative caption is combined to find the target person among gallery images. As shown in the bottom of Figure 2, the query consists of two parts: an image and a textual caption. The image query passes through the visual encoder and the TINet  $f_M$  sequentially to obtain the inverted word  $S_*$ . Then, the query information is concatenated by using a sentence template "a  $[S_*]$  is {Caption}", and finally, the concatenated sentence serves as a text query to search for the target image in the gallery. Note that our approach is highly flexible during both training and testing phases, making it easy to strike a balance between performance and efficiency in real-world applications, and we discuss it in detail in the supplementary materials.

## 4 ITCPR DATASET

In contrast to existing CIR datasets [30, 45], where reference and target images only need to be loosely related, the CPR datasets subject to the constraint that both of them depict the same person. Therefore, when constructing the ITCPR dataset, we ask the selected images to have the same identity, but wear different clothes

**Table 1: Zero-shot retrieval results of relevant methods on the ITCPR dataset.  $\mathcal{L}_{Vis}$  and  $\mathcal{L}_{Text}$  represent the losses used for supervised optimization of the TINet. The † symbol indicates that the training of the methods was performed on the original pre-trained parameters of CLIP, which may pose challenges for domain generalization and result in certain performance degradation.**

No.	Backbone	Dual Encoder	Method	Rank-1	Rank-5	Rank-10	mAP
1	ViT-B/16	CLIP [37]	Image-only	7.357	16.803	22.934	12.524
2			Text-only	4.632	10.309	14.759	8.116
3			Image+Text	16.757	32.516	40.372	24.674
4		Fine-tuned	Image-only	5.041	10.763	13.442	8.086
5			Text-only	26.385	46.458	56.267	36.132
6			Image+Text	29.837	50.136	59.037	39.632
7			Text+Model C [11]	32.743	55.904	64.487	43.484
8			<b>Ours (<math>\mathcal{L}_{Vis}</math>)</b>	38.919	59.310	67.075	48.538
9			<b>Ours (<math>\mathcal{L}_{Text}</math>)</b>	<u>40.054</u>	<u>61.262</u>	<u>68.574</u>	<u>49.903</u>
10			<b>Ours (<math>\mathcal{L}_{Vis} + \mathcal{L}_{Text}</math>)</b>	<b>40.872</b>	<b>61.989</b>	<b>68.847</b>	<b>50.521</b>
11	ViT-L/14	CLIP [37]	Image-only	8.265	18.483	24.523	13.795
12			Text-only	3.270	9.219	14.532	6.929
13			Image+Text	18.165	35.195	43.324	26.652
14			Pic2Word [38]	21.208	37.148	44.505	29.108
15			SEARLE-XL [2]	22.252	37.693	45.232	30.543
16		Fine-tuned	Image-only	5.268	10.763	13.987	8.345
17			Text-only	28.974	50.817	59.900	39.333
18			Image+Text	32.016	52.634	60.990	41.831
19			Text+Model C [11]	35.377	53.588	61.172	44.084
20			Pic2Word [38] †	32.652	55.041	62.807	43.086
21			SEARLE-XL [2] †	33.379	54.496	62.943	43.333
22			<b>Ours (<math>\mathcal{L}_{Vis}</math>)</b>	43.960	64.714	72.480	53.554
23			<b>Ours (<math>\mathcal{L}_{Text}</math>)</b>	<u>45.549</u>	<u>66.803</u>	<u>74.796</u>	<u>55.260</u>
24	<b>Ours (<math>\mathcal{L}_{Vis} + \mathcal{L}_{Text}</math>)</b>	<b>45.913</b>	<b>66.848</b>	<b>75.114</b>	<b>55.630</b>		

or be in different scenes. In our implementation, publicly available clothes-changing datasets such as Celeb-reid [18], PRCC [49], and LAST [40] are utilized as our image sources.

The annotation process consists of several steps. The first step involves obtaining identities that have multiple images with different clothes to provide a diverse selection in subsequent steps. Next, two images are selected from the ones associated with each chosen identity and are denoted as  $I_q$  and  $I_t$ . Annotations that exclusively capture the distinctions between  $I_q$  and  $I_t$ , denoted as  $T_q$ , are manually crafted. Note that, the two images should ideally characterize partially matching costume, allowing  $I_q$  to provide additional clothing-related information beyond facial features and body posture. This additional clothing information will not be mentioned in annotation  $T_q$ , ensuring that CPR methods can only correctly identify  $I_t$  by making use of both  $I_q$  and  $T_q$ . After that, we obtain multiple triplets  $(I_q, T_q, I_t)$  for composed person retrieval. To prevent false negative cases, the gallery images are screened and re-annotated in the dataset (Supplementary B.1 for details). Some examples of ITCPR dataset are illustrated in Figure 3.

In summary, ITCPR comprises a total of 2,225 annotated triplets. These triplets encompass 2,202 unique combinations  $(I_q, T_q)$  as queries. ITCPR contains 1,151 images and 512 identities from Celeb-reID [18], 146 images and 146 identities from PRCC [49], and 905 images and 541 identities from LAST [40]. In the target gallery, there are a total of 20,510 images of persons from the three datasets, with 2,225 corresponding ground truths for the queries. The mentioned

annotations are exclusively designated for testing in the ZS-CPR task, which expects to achieve substantial performance without utilizing any data from the three datasets mentioned above.

## 5 EXPERIMENTS

### 5.1 Experiments Setup

**Datasets.** The Word4Per method employs image-caption datasets for both fine-tuning and TINet training (where  $\mathcal{L}_{Vis}$  only uses images). In this part, the image-caption dataset CUHK-PEDES [25] is used as the default training dataset.

**Implementation Details.** The experiments are conducted on a single A100 GPU. The input image size is adjusted to  $384 \times 128$ , with each image patch measuring  $16 \times 16$ . The maximum length for text tokens is set to 77. Training is performed by the Adam [21] optimizer for 60 epochs, with a batch size of 128. Cosine learning rate decay is applied. Initially, 5 warm-up epochs are conducted, gradually increasing the learning rate from 1/10 of the initial learning rate to the initial value. The temperature parameter  $\tau$  in the losses is set to 0.02.

During the fine-tuning, the image and text encoders are initialized with pretrained CLIP [37] parameters. The initial learning rate is set to  $10^{-5}$ . For modules with random initialization, the initial learning rate is set to  $5 \times 10^{-5}$ . In the training of the TINet, the parameters of the visual and text encoder inherit the fine-tuned parameters and remain frozen. A fully connected neural network is



used to construct a lightweight TINet. When the visual encoder is ViT-B/16, the input and output dimensions are set to 512. When it is ViT-L/14, the input and output dimensions are 768, while the hidden layer dimension remains at 512. The parameters are randomly initialized. The initial learning rate is set to  $10^{-4}$ . The CUHK-PEDES dataset is used for training, and if the visual encoder is ViT-B/16, the training takes approximately 2 hours, and if is ViT-L/14, the training takes about 5 hours.

**Evaluation Metrics.** For ZS-CPR testing metrics, performance is evaluated by the Rank-k measure. This measure is employed to assess the probability of finding at least one matching person image among the top-k similar candidates for given query. Common values for k are 1, 5, and 10. Higher Rank-k scores indicate that the system effectively retrieves targets. In addition, we also employ the mean average precision (mAP) for evaluation. mAP is computed by calculating the average precision of retrieved relevant images and averaging the results across all queries, considering the performance of model on various queries. Higher Rank-k and mAP values signify superior method performance.

## 5.2 Quantitative Results

Word4Per is compared with several baseline methods [37] that support zero-shot retrieval, as well as Pic2Word [38] and SEARLE [2], methods with notable performance in the ZS-CIR task. The baseline methods include several testing modes: 1) Image-only: using only the reference image via a pre-trained visual encoder to retrieve person. 2) Text-only: using only relative caption via a pre-trained text encoder. 3) Image + Text: Target person retrieval by averaging features obtained from the above two methods. 4) Text+*Model C*: Target person retrieval by averaging results obtained from the Text-only and *Model C* (Simple-CCReID [11] is trained on the LTCC [35] dataset to prevent data leakage). 5) CIR methods [2, 38]: using the parameters of the TINet trained with the original CIR method. Our method is trained and tested on both ViT-B/16 and ViT-L/14 visual encoders. Because Pic2Word and SEARLE are only provided for the ViT-L/14 scheme, thus we conduct the comparison with them only under the ViT-L/14 experimental setting.

Table 1 shows the test results of comparative methods on the ITCPR dataset, demonstrating that our method significantly outperforms all baseline models and ZS-CIR methods. The experimental results of No. 1-6, No. 11-13, and No. 16-18 reveal that utilizing both text and image information, regardless of whether the encoder is trained with CLIP [37] or fine-tuning, leads to optimal performance. These results also show the rational construction of our ITCPR dataset, leveraging both textual and visual cues from the query, the target person can be effectively identified. Comparing with the results of experiments No. 1-3 with No. 4-6, and No. 11-13 with No. 16-18, it is evident that fine-tuning the dual encoders is effective and necessary. Specifically, the results of No. 7 and No. 19 demonstrate that our method significantly outperforms the dual-model approach incorporating clothes-changing models with a lower computational cost. Moreover, the results of No. 8-10 and No. 22-24 indicate that supervising the TINet with  $\mathcal{L}_{Text}$  is more effective, and a combination of both supervisions achieves the best performance (Supplementary C for further results).

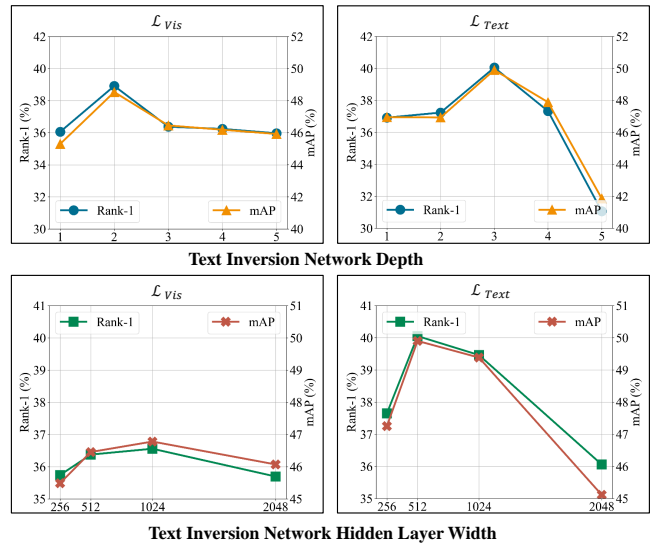


**Figure 4: Method performance using TINet with different depths and hidden layer widths under various supervisions. Top: Performance using TINet with different depths, with a hidden layer width of 512. Bottom: Performance using TINet with different hidden layer widths, all with a depth of three layers.**

## 5.3 Ablation Studies

To further show the effectiveness of the proposed Word4Per method for the ZS-CPR problem, we conduct extensive ablation studies. Due to limited training resources, the majority of ablation experiments are conducted on the fine-tuned dual encoders with a visual encoder of ViT-B/16. Note that experiments without specifying the dual encoders are based on this setup, and the parameters of the encoders are obtained from the fine-tuning network and remain frozen.

**Ablation study for TINet architecture.** Figure 4 illustrates the performance of TINets with different depths and hidden layer widths under various supervisions. For  $\mathcal{L}_{Vis}$  supervision, a two-layer fully connected neural network emerges as the optimal structure. On the other hand, for  $\mathcal{L}_{Text}$  supervision, a three-layer fully connected neural network is found to be most suitable. The hidden layer width exhibits sensitivity primarily to  $\mathcal{L}_{Text}$  supervision, with the optimal width being 512 units. In the quest for a harmonious balance between efficiency and precision, we opt to maintain a consistent hidden layer width of 512 across different configurations.

**Ablation study for Pseudo-word ( $S_*$ ).** Employing various templates for  $S_*$  and altering token length results in distinct performance, as shown in Table 2. Comparative analysis of results No. 1-3 reveals that, compared to directly appending relative captions to  $S_*$ , utilizing intuitively coherent templates can enhance performance. Furthermore, experimental results No. 3-6 indicate that when the token length of  $S_*$  is fewer than four, performance remains relatively stable but declines with longer token lengths due to the detrimental impact of excessive inversion elements on linguistic stability.

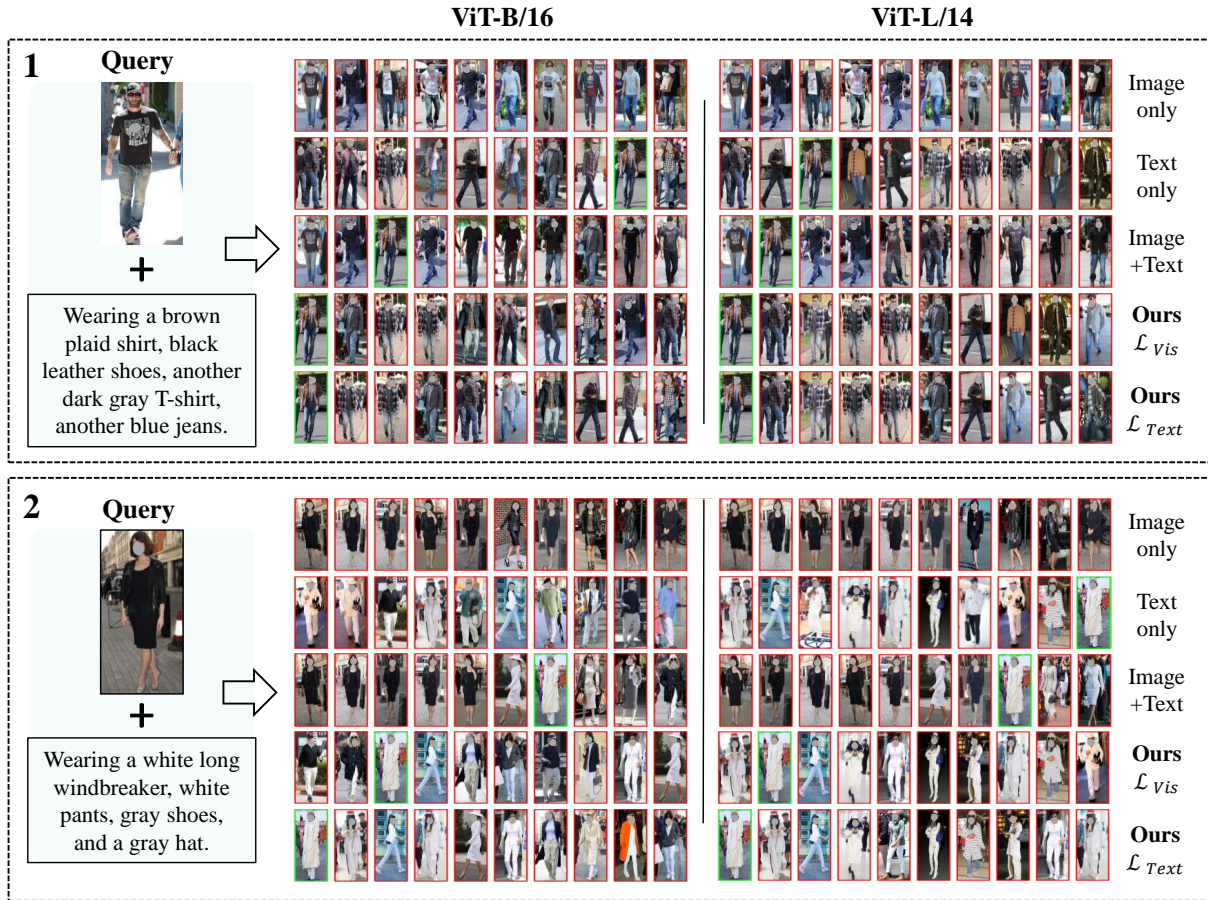


Figure 5: Top-10 retrieval results on the ITCPR dataset for relevant methods. The figure presents retrieval results for two query examples under different methods, all employing fine-tuned encoders.

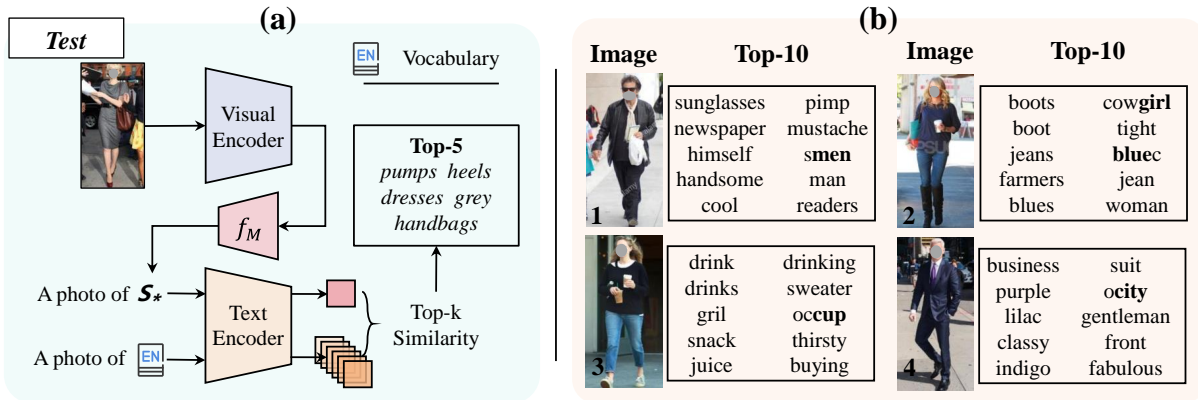


Figure 6: (a) Semantic information exploration of pseudo-word tokens. Experiments are conducted using the  $\mathcal{L}_{Text}$  supervised optimized TINet (ViT-B/16). (b) Top-10 vocabulary words most similar to pseudo-words in some images.

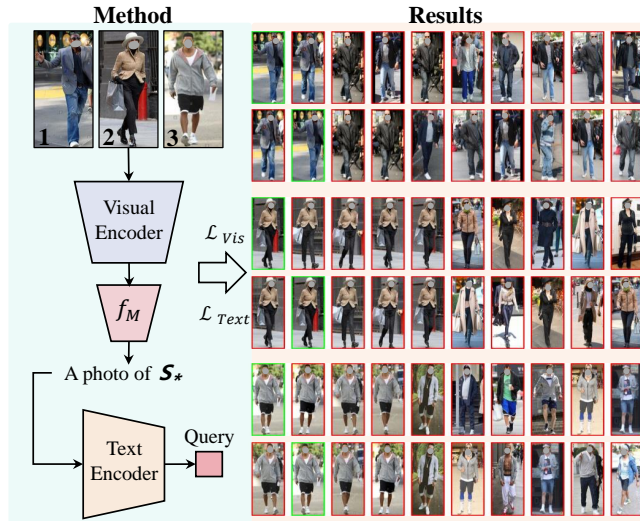
Therefore, considering all the factors above, the configuration of experiment No. 3 is chosen as the final setup.

### 5.4 Qualitative Results

The visualization of the results obtained by ZS-CPR models are compared. Figure 5 shows two typical cases. In case 1, it is evident

**Table 2: Template and token length of  $S_*$  impact on performance. Supervised optimization is conducted with  $\mathcal{L}_{Text}$ .**

No.	Template	Length	R1	R5	R10	mAP
1	$[S_*]$ {Caption}	1	39.055	60.263	67.802	48.995
2	$[S_*]$ is {Caption}	1	39.555	60.490	68.211	49.266
3	$a [S_*]$ is {Caption}	1	<b>40.054</b>	<b>61.262</b>	<b>68.574</b>	<b>49.903</b>
4	$a [S_*]$ is {Caption}	2	<b>40.100</b>	60.990	68.074	49.708
5	$a [S_*]$ is {Caption}	4	39.691	<u>61.126</u>	<b>69.028</b>	<u>49.734</u>
6	$a [S_*]$ is {Caption}	8	38.193	59.083	66.258	47.929

**Figure 7: Method and results of pseudo-word token retrieval for the original image. On the left is an illustration of the retrieval method, and on the right are the retrieval results for three examples.**

that, regardless of the parameters scale, using image-only retrieval yields the poorest results. Because it trends to obtain the images possessing visually similar pixel distributions, and the dataset contains numerous instances of clothes-changing, resulting in subpar performance. Text-only retrieval also falls short of expectations since most annotations in the dataset describe attire briefly, and there are numerous images with similar clothing. The combined use of both modalities in retrieval often yields the desired target images among the top results. When using the Word4Per method, the TINet, supervised with either  $\mathcal{L}_{Text}$  or  $\mathcal{L}_{Vis}$ , consistently succeeds in finding the target image. case 2 exhibits a similar pattern to case 1. However, in scenarios where the training dataset is unfiltered and remains consistent, the ambiguity of vision negatively effects the effectiveness of the model. In contrast, the textual information is more stable than visual one, thus TINet optimized with  $\mathcal{L}_{Text}$  tend to achieve the best retrieval results.

To demonstrate the effectiveness of the pseudo-word tokens generated by the TINet in capturing image information, another comparative experiment is conducted, as shown in Figure 7. In this experiment, the pseudo-word tokens from all reference images

**Table 3: Experimental results of replacing pseudo-word tokens with existing words. “1st Sim” indicates using words with the highest similarity to replace pseudo-word tokens for target retrieval.**

No.	Backbone	Method	Rank-1	Rank-5	Rank-10	mAP
1	ViT-B/16	Text-only	26.385	46.458	56.267	36.132
2		1st Sim	27.884	49.001	57.856	37.955
3		$\mathcal{L}_{Text}$	<b>40.054</b>	<b>61.262</b>	<b>68.574</b>	<b>49.903</b>
4	ViT-L/14	Text-only	28.974	50.817	59.900	39.333
5		1st Sim	32.016	53.769	62.761	42.242
6		$\mathcal{L}_{Text}$	<b>45.549</b>	<b>66.803</b>	<b>74.796</b>	<b>55.260</b>

are used to perform retrievals on a mixed dataset containing all reference images and gallery images. When employing the TINet supervised with  $\mathcal{L}_{Vis}$ , the model consistently finds the original image from the most similar retrieval results, even in situations where appearance of a person is highly consistent, as it leverages differences in the background. However, supervising with  $\mathcal{L}_{Text}$ , the original image cannot be located among the most similar retrieval results. This is mainly because semantic annotations for person images often do not focus on the background, but instead emphasize characteristics related to the individuals. It is also a key reason for obtaining promising performance for the ZS-CPR task.

## 6 DISCUSSION

Based on above results, it is evident that a well-trained TINet can effectively transform the image into a single pseudo-word token and can concisely and efficiently combine the relative caption to improve CPR performance. However, what semantic information is contained in these pseudo-words and whether they can be replaced with real words from the vocabulary? To address these questions, within the entire vocabulary we find the words that are most similar to the pseudo-words, so as to infer the relevant semantic information hidden in the pseudo-words (Figure 6(a)).

Several results with randomly chosen images are shown in Figure 6(b). It becomes apparent that words similar to the pseudo-words can effectively describe the original image, containing various details about the person. These details include gender information (e.g., *man*, *woman*, *girl*), clothing details (e.g., *boots*, *sweater*, *suit*), color descriptions (e.g., *blue*, *purple*, *indigo*), and items carried by the pedestrian (e.g., *newspaper*, *sunglasses*, *handbags*). Furthermore, the obtained words contain additional aspects, such as the state of the persons, style, spatial location, attire materials, etc. It is worth noting that, some vocabulary may not directly describe the image, but certain parts of these words (bolded in the Figure 6(b)) can be prompted to the corresponding image. This phenomenon may be owned to the usage of Byte Pair Encoding (BPE) [39] in the text encoding. By extending observation to top-50 even top-100 words, we can unearth more meaningful semantic information. This suggests that pseudo-word tokens obtained by the TINet are actually a combination of multiple meaningful semantic information and contain a variety of information.

If pseudo-word tokens are replaced with the most similar words from the vocabulary, will the results still be stable? To investigate this, relevant experiments are conducted, and the results are shown



in Table 3. The results show although adding a valid word can bring some performance improvement, it is far less obvious than the use of pseudo-word tokens. The results are also quite comprehensible, that is, it is challenging to summarize a person image just using one existing word, whereas one pseudo-word token can accomplish this.

## 7 CONCLUSION

In this paper, we address limitations in handling queries that involve both image and text information for person retrieval, through the introduction of CPR task. To overcome data annotation challenges in CPR, we put forward the ZS-CPR problem, eliminating reliance on expensive triplet annotations. Furthermore, a two-stage framework called Word4Per is developed to train ZS-CPR model, achieving very promising performance on our proposed ITCPR dataset without the need for CPR datasets. Comprehensive ablation studies are also conducted on Word4Per, and a slice of valuable insights are obtained.

However, The proposed CPR task is still in its infancy, and there are many directions that can be optimized. For instance, our method does not explicitly focus on maintaining consistent facial and body features for the same person. In addition, narrowing the retrieval scope based on this information without sacrificing retrieval efficiency is also a valuable issue.

## REFERENCES

- [1] Aishwarya Agrawal, Jiasen Lu, Stanislaw Antol, Margaret Mitchell, C. Lawrence Zitnick, Dhruv Batra, and Devi Parikh. 2015. VQA: Visual Question Answering. *arXiv: Computation and Language*, arXiv: Computation and Language (May 2015).
- [2] Alberto Baldrati, Lorenzo Agnolucci, Marco Bertini, and Alberto Del Bimbo. 2023. Zero-Shot Composed Image Retrieval with Textual Inversion. *arXiv preprint arXiv:2303.15247* (2023).
- [3] Tianlong Chen, Shaojin Ding, Jingyi Xie, Ye Yuan, Wuyang Chen, Yang Yang, Zhou Ren, and Zhiyong Wang. 2019. ABD-Net: Attentive but Diverse Person Re-Identification. In *2019 IEEE/CVF International Conference on Computer Vision (ICCV)*. <https://doi.org/10.1109/iccv.2019.00844>
- [4] Yanbei Chen, Shaogang Gong, and Loris Bazzani. 2020. Image Search With Text Feedback by Visiolinguistic Attention Learning. In *2020 IEEE/CVF Conference on Computer Vision and Pattern Recognition (CVPR)*. <https://doi.org/10.1109/cvpr42600.2020.00307>
- [5] Yuhao Chen, Guoqing Zhang, Yujiang Lu, Zhenxing Wang, and Yuhui Zheng. 2022. Tipcb: A simple but effective part-based convolutional baseline for text-based person search. *Neurocomputing* 494 (2022), 171–181.
- [6] Marcella Cornia, Matteo Stefanini, Lorenzo Baraldi, and Rita Cucchiara. 2020. Meshed-Memory Transformer for Image Captioning. In *2020 IEEE/CVF Conference on Computer Vision and Pattern Recognition (CVPR)*. <https://doi.org/10.1109/cvpr42600.2020.01059>
- [7] Jacob Devlin, Ming-Wei Chang, Kenton Lee, and Kristina Toutanova. 2018. Bert: Pre-training of deep bidirectional transformers for language understanding. *arXiv preprint arXiv:1810.04805* (2018).
- [8] Zefeng Ding, Changxing Ding, Zhiyin Shao, and Dacheng Tao. 2021. Semantically self-aligned network for text-to-image part-aware person re-identification. *arXiv preprint arXiv:2107.12666* (2021).
- [9] Rinon Gal, Yuval Alaluf, Yuval Atzmon, Or Patashnik, Amit Haim Bermano, Gal Chechik, and Daniel Cohen-or. 2022. An Image is Worth One Word: Personalizing Text-to-Image Generation using Textual Inversion. In *The Eleventh International Conference on Learning Representations*.
- [10] Douglas Gray and Hai Tao. 2008. Viewpoint invariant pedestrian recognition with an ensemble of localized features. In *Computer Vision—ECCV 2008: 10th European Conference on Computer Vision, Marseille, France, October 12–18, 2008, Proceedings, Part I 10*. Springer, 262–275.
- [11] Xinqian Gu, Hong Chang, Bingpeng Ma, Shutao Bai, Shiguang Shan, and Xilin Chen. 2022. Clothes-changing person re-identification with rgb modality only. In *Proceedings of the IEEE/CVF Conference on Computer Vision and Pattern Recognition*. 1060–1069.
- [12] Xiaoxiao Guo, Hui Wu, Yu Cheng, StevenJ. Rennie, Gerald Tesauro, and Rogerio Feris. 2018. Dialog-based Interactive Image Retrieval. *arXiv: Computer Vision and Pattern Recognition*, arXiv: Computer Vision and Pattern Recognition (May 2018).
- [13] Kaiming He, Xiangyu Zhang, Shaoqing Ren, and Jian Sun. 2016. Deep residual learning for image recognition. In *Proceedings of the IEEE conference on computer vision and pattern recognition*. 770–778.
- [14] Shuting He, Hao Luo, Pichao Wang, Fan Wang, Hao Li, and Wei Jiang. 2021. TransReID: Transformer-based Object Re-Identification. In *2021 IEEE/CVF International Conference on Computer Vision (ICCV)*. <https://doi.org/10.1109/iccv48922.2021.01474>
- [15] Alexander Hermans, Lucas Beyer, and Bastian Leibe. 2017. In Defense of the Triplet Loss for Person Re-Identification. *arXiv: Computer Vision and Pattern Recognition*, arXiv: Computer Vision and Pattern Recognition (Mar 2017).
- [16] Martin Hirzer, Csaba Beleznai, Peter M Roth, and Horst Bischof. 2011. Person re-identification by descriptive and discriminative classification. In *Image Analysis: 17th Scandinavian Conference, SCIA 2011, Ystad, Sweden, May 2011. Proceedings 17*. Springer, 91–102.
- [17] Mehrdad Hosseinzadeh and Yang Wang. 2020. Composed Query Image Retrieval Using Locally Bounded Features. In *2020 IEEE/CVF Conference on Computer Vision and Pattern Recognition (CVPR)*. <https://doi.org/10.1109/cvpr42600.2020.00365>
- [18] Yan Huang, Qiang Wu, Jingsong Xu, and Yi Zhong. 2019. Celebrities-reid: A benchmark for clothes variation in long-term person re-identification. In *2019 International Joint Conference on Neural Networks (IJCNN)*. IEEE, 1–8.
- [19] Mengxi Jia, Xinhua Cheng, Shijian Lu, and Jian Zhang. 2022. Learning disentangled representation implicitly via transformer for occluded person re-identification. *IEEE Transactions on Multimedia* 25 (2022), 1294–1305.
- [20] Ding Jiang and Mang Ye. 2023. Cross-Modal Implicit Relation Reasoning and Aligning for Text-to-Image Person Retrieval. In *Proceedings of the IEEE/CVF Conference on Computer Vision and Pattern Recognition*. 2787–2797.
- [21] Diederik P. Kingma and Jimmy Ba. 2014. Adam: A Method for Stochastic Optimization. *arXiv: Learning*, arXiv: Learning (Dec 2014).
- [22] Seungmin Lee, Dongwan Kim, and Bohyung Han. 2021. CoSMo: Content-Style Modulation for Image Retrieval with Text Feedback. In *2021 IEEE/CVF Conference on Computer Vision and Pattern Recognition (CVPR)*. <https://doi.org/10.1109/cvpr46437.2021.00086>
- [23] Hanjun Li, Gaojie Wu, and Wei-Shi Zheng. 2021. Combined Depth Space based Architecture Search For Person Re-identification. In *2021 IEEE/CVF Conference on Computer Vision and Pattern Recognition (CVPR)*. <https://doi.org/10.1109/cvpr46437.2021.00666>
- [24] Junnan Li, Dongxu Li, Caiming Xiong, and Steven Hoi. 2022. Blip: Bootstrapping language-image pre-training for unified vision-language understanding and generation. In *International Conference on Machine Learning*. PMLR, 12888–12900.
- [25] Shuang Li, Tong Xiao, Hongsheng Li, Bolei Zhou, Dayu Yue, and Xiaogang Wang. 2017. Person search with natural language description. In *Proceedings of the IEEE conference on computer vision and pattern recognition*. 1970–1979.
- [26] Wei Li and Xiaogang Wang. 2013. Locally aligned feature transforms across views. In *Proceedings of the IEEE conference on computer vision and pattern recognition*. 3594–3601.
- [27] Wei Li, Rui Zhao, Tong Xiao, and Xiaogang Wang. 2014. Deepreid: Deep filter pairing neural network for person re-identification. In *Proceedings of the IEEE conference on computer vision and pattern recognition*. 152–159.
- [28] Yulin Li, Jianfeng He, Tianzhu Zhang, Xiang Liu, Yongdong Zhang, and Feng Wu. 2021. Diverse part discovery: Occluded person re-identification with part-aware transformer. In *Proceedings of the IEEE/CVF Conference on Computer Vision and Pattern Recognition*. 2898–2907.
- [29] Delong Liu and Haiwen Li. 2023. Unleashing the Imagination of Text: A Novel Framework for Text-to-image Person Retrieval via Exploring the Power of Words. *arXiv preprint arXiv:2307.09059* (2023).
- [30] Zheyuan Liu, Cristian Rodriguez-Opazo, Damien Teney, and Stephen Gould. 2021. Image Retrieval on Real-life Images with Pre-trained Vision-and-Language Models. In *2021 IEEE/CVF International Conference on Computer Vision (ICCV)*. <https://doi.org/10.1109/iccv48922.2021.00213>
- [31] Chen Change Loy, Tao Xiang, and Shaogang Gong. 2009. Multi-camera activity correlation analysis. In *2009 IEEE Conference on Computer Vision and Pattern Recognition*. IEEE, 1988–1995.
- [32] Hao Luo, Youzhi Gu, Xingyu Liao, Shenqi Lai, and Wei Jiang. 2019. Bag of tricks and a strong baseline for deep person re-identification. In *Proceedings of the IEEE/CVF conference on computer vision and pattern recognition workshops*. 0–0.
- [33] Jingjing Qian, Wei Jiang, Hao Luo, and Hongyan Yu. 2020. Stripe-based and attribute-aware network: a two-branch deep model for vehicle re-identification. *Measurement Science and Technology* (Sep 2020), 095401. <https://doi.org/10.1088/1361-6501/ab8b81>
- [34] Xuelin Qian, Wenxuan Wang, Li Zhang, Fangrui Zhu, Yanwei Fu, Tao Xiang, Yu-Gang Jiang, and Xiangyang Xue. 2020. Long-term cloth-changing person re-identification. In *Proceedings of the Asian Conference on Computer Vision*.
- [35] Xuelin Qian, Wenxuan Wang, Li Zhang, Fangrui Zhu, Yanwei Fu, Tao Xiang, Yu-Gang Jiang, and Xiangyang Xue. 2020. Long-term cloth-changing person re-identification. In *Proceedings of the Asian Conference on Computer Vision*.
- [36] Ruijie Quan, Xuanyi Dong, Yu Wu, Linchao Zhu, and Yi Yang. 2019. Auto-ReID: Searching for a Part-aware ConvNet for Person Re-Identification. In *2019 IEEE/CVF International Conference on Computer Vision (ICCV)*. <https://doi.org/10.1109/iccv48922.2019.00086>

- 1109/iccv.2019.00385
- [37] Alec Radford, Jong Wook Kim, Chris Hallacy, Aditya Ramesh, Gabriel Goh, Sandhini Agarwal, Girish Sastry, Amanda Askell, Pamela Mishkin, Jack Clark, et al. 2021. Learning transferable visual models from natural language supervision. In *International conference on machine learning*. PMLR, 8748–8763.
- [38] Kuniaki Saito, Kihyuk Sohn, Xiang Zhang, Chun-Liang Li, Chen-Yu Lee, Kate Saenko, and Tomas Pfister. 2023. Pic2word: Mapping pictures to words for zero-shot composed image retrieval. In *Proceedings of the IEEE/CVF Conference on Computer Vision and Pattern Recognition*. 19305–19314.
- [39] Rico Sennrich, Barry Haddow, and Alexandra Birch. 2015. Neural machine translation of rare words with subword units. *arXiv preprint arXiv:1508.07909* (2015).
- [40] Xiujun Shu, Xiao Wang, Xianghao Zang, Shiliang Zhang, Yuanqi Chen, Ge Li, and Qi Tian. 2021. Large-scale spatio-temporal person re-identification: Algorithms and benchmark. *IEEE Transactions on Circuits and Systems for Video Technology* 32, 7 (2021), 4390–4403.
- [41] Yifan Sun, Liang Zheng, Yi Yang, Qi Tian, and Shengjin Wang. 2018. *Beyond Part Models: Person Retrieval with Refined Part Pooling (and a Strong Convolutional Baseline)*. 501–518. [https://doi.org/10.1007/978-3-030-01225-0\\_30](https://doi.org/10.1007/978-3-030-01225-0_30)
- [42] Ashish Vaswani, Noam Shazeer, Niki Parmar, Jakob Uszkoreit, Llion Jones, AidanN. Gomez, Lukasz Kaiser, and Illia Polosukhin. 2017. Attention is All you Need. *Neural Information Processing Systems, Neural Information Processing Systems* (Jun 2017).
- [43] Pingyu Wang, Zhicheng Zhao, Fei Su, and Honying Meng. 2022. LTRelD: Factorizable Feature Generation with Independent Components for Long-Tailed Person Re-Identification. *IEEE Transactions on Multimedia* (2022).
- [44] Longhui Wei, Shiliang Zhang, Wen Gao, and Qi Tian. 2018. Person transfer gan to bridge domain gap for person re-identification. In *Proceedings of the IEEE conference on computer vision and pattern recognition*. 79–88.
- [45] Hui Wu, Yupeng Gao, Xiaoxiao Guo, Ziad Al-Halah, Steven Rennie, Kristen Grauman, and Rogerio Feris. 2021. Fashion IQ: A New Dataset Towards Retrieving Images by Natural Language Feedback. In *2021 IEEE/CVF Conference on Computer Vision and Pattern Recognition (CVPR)*. <https://doi.org/10.1109/cvpr46437.2021.01115>
- [46] Yushuang Wu, Zizheng Yan, Xiaoguang Han, Guanbin Li, Changqing Zou, and Shuguang Cui. 2021. LapsCore: language-guided person search via color reasoning. In *Proceedings of the IEEE/CVF International Conference on Computer Vision*. 1624–1633.
- [47] Tong Xiao, Shuang Li, Bochao Wang, Liang Lin, and Xiaogang Wang. 2016. End-to-end deep learning for person search. *arXiv preprint arXiv:1604.01850* 2, 2 (2016), 4.
- [48] Peng Xu and Xiatian Zhu. 2023. DeepChange: A Long-Term Person Re-Identification Benchmark with Clothes Change. In *Proceedings of the IEEE/CVF International Conference on Computer Vision*. 11196–11205.
- [49] Qize Yang, Ancong Wu, and Wei-Shi Zheng. 2019. Person re-identification by contour sketch under moderate clothing change. *IEEE transactions on pattern analysis and machine intelligence* 43, 6 (2019), 2029–2046.
- [50] Yan Zhang, Binyu He, Li Sun, and Qingli Li. 2021. Progressive Multi-Stage Feature Mix for Person Re-Identification. In *ICASSP 2021 - 2021 IEEE International Conference on Acoustics, Speech and Signal Processing (ICASSP)*. <https://doi.org/10.1109/icassp39728.2021.9413533>
- [51] Ying Zhang and Huchuan Lu. 2018. Deep cross-modal projection learning for image-text matching. In *Proceedings of the European conference on computer vision (ECCV)*. 686–701.
- [52] Zhizheng Zhang, Cuiling Lan, Wenjun Zeng, Xin Jin, and Zhibo Chen. 2019. Relation-Aware Global Attention for Person Re-identification. *arXiv: Computer Vision and Pattern Recognition, arXiv: Computer Vision and Pattern Recognition* (Apr 2019).
- [53] Liang Zheng, Liyue Shen, Lu Tian, Shengjin Wang, Jingdong Wang, and Qi Tian. 2015. Scalable person re-identification: A benchmark. In *Proceedings of the IEEE international conference on computer vision*. 1116–1124.
- [54] WS Zheng. 2009. S. Gong, and T. Xiang, "Associating groups of people," *BMVC* (2009).
- [55] Zhedong Zheng, Liang Zheng, Michael Garrett, Yi Yang, Mingliang Xu, and Yi-Dong Shen. 2020. Dual-path convolutional image-text embeddings with instance loss. *ACM Transactions on Multimedia Computing, Communications, and Applications (TOMM)* 16, 2 (2020), 1–23.
- [56] Kaiyang Zhou, Yongxin Yang, Andrea Cavallaro, and Tao Xiang. 2019. Omni-Scale Feature Learning for Person Re-Identification. In *2019 IEEE/CVF International Conference on Computer Vision (ICCV)*. <https://doi.org/10.1109/iccv.2019.00380>
- [57] Aichun Zhu, Zijie Wang, Yifeng Li, Xili Wan, Jing Jin, Tian Wang, Fangqiang Hu, and Gang Hua. 2021. Dssl: Deep surroundings-person separation learning for text-based person retrieval. In *Proceedings of the 29th ACM International Conference on Multimedia*. 209–217.

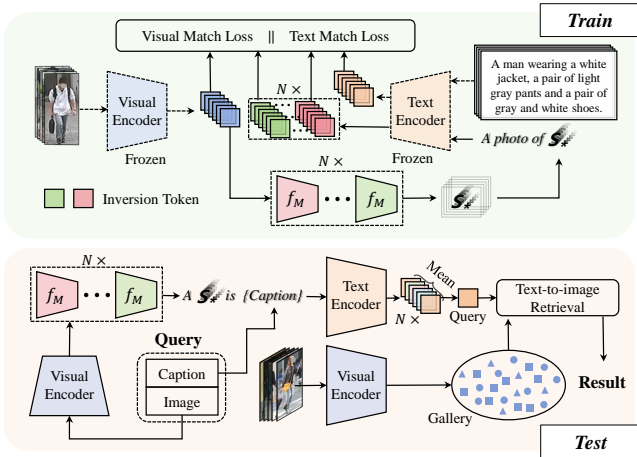


Figure A: Flexibility in Training and Inference. Top: The flexibility of the TINet training process allows the simultaneous and independent training of any number of  $f_M$  networks with different structures and loss supervision optimizations, using the same dataset. Bottom: The flexibility during the inference stage allows the combination of any number of TINet, regardless of their optimization process.

## A FLEXIBILITY IN TRAINING AND TESTING.

Word4Per exhibits the flexibility both in training and testing phases. As shown in Figure A, during the training of the TINet, under the condition that the input data keeps consistent, multiple TINets  $f_M$  can be learnt simultaneously. Each  $f_M$  can be configured flexibly in terms of its structure and associated loss functions. Since the parameters of the visual encoder and text encoder remain frozen, each  $f_M$  will be updated solely based on respective loss function. This mode allows to share the frozen dual encoders in a single training process, reducing the number of times that the images and texts in the dataset pass through the encoders independently, enhancing efficiency.

During testing, our method becomes even more flexible. For example, it allows different number of networks with various structures, loss optimizations, and training data. After an image passes through the visual encoder, it can be processed by multiple TINets  $f_M$  to obtain multiple pseudo-words  $S_*$ , resulting in multiple final queries, whose average can yield the final query embedding and the corresponding retrieval result. In general, using more TINets can lead to better performance but lower efficiency. Therefore, different application requirements can find the balance between accuracy and efficiency.

## B ADDITIONAL DETAILS

### B.1 ITCPR Datasets Re-annotation

A large number of noise images in gallery can potentially introduce false negative images. For example, for certain queries, some images could be potential ground truth but remain unlabeled. Incorporating such cases will decrease the reliability of the evaluation metrics. Therefore, as shown in Figure B, after completing the dataset annotation and adding noise images to the image gallery,

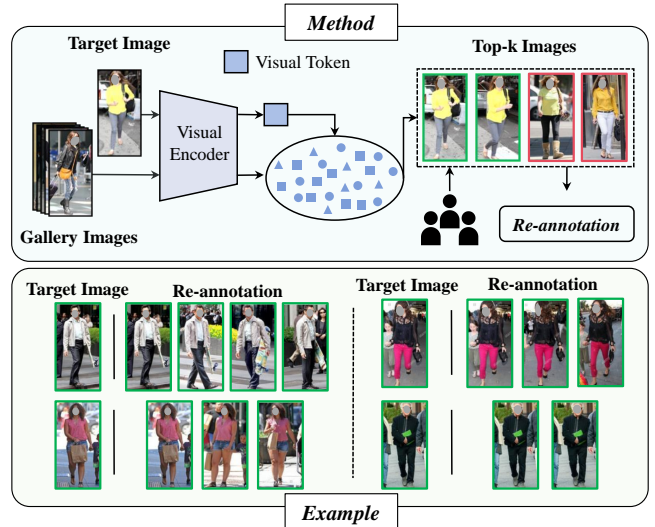


Figure B: False negative elimination scheme in ITCPR. Top: The method of eliminating false negative images and adding annotations in the dataset. Bottom: Examples of false negative images re-annotated in ITCPR.

we employ a well-trained visual encoder to search for the most similar images for each target image, followed by manual verification. By this way, we add corresponding annotations to eliminate false negatives, and the ITCPR dataset has been refined.

### B.2 Other Datasets

**Image-Caption Datasets.** Notably, there are three publicly accessible datasets: CUHK-PEDES [25], ICFG-PEDES [8], and RSTPReid [57]. Our primary concern focuses on the CUHK-PEDES dataset, while the other two datasets are mainly employed for ablation experiments. In the subsequent experiments (C.5), we abbreviate datasets as follows, CUHK-PEDES is denoted as  $C$ , ICFG-PEDES as  $I$ , and RSTPReid as  $R$ .

**Image Datasets.** In the Word4Per method, when exclusively utilizing  $\mathcal{L}_{Vis}$  for textual inversion optimization, the training uses the datasets containing only images. It's essential to mention that datasets containing images of persons are abundant and widely available in IPR, including Market1501 [53], MSMT17 [44], CUHK02 [26], CUHK03-NP [27], CUHK-SYSU [47], GRID [31], VIPeR [10], QMUL i-LIDS [54], and PRID [16]. In subsequent ablation experiments, we combine above datasets with the images from image-caption datasets mentioned before to yield a total of 1,057,361 images, is collectively called the IPR dataset.

### B.3 Image-Caption Dataset Details

CUHK-PEDES [25] comprises a total of 40,206 images and 80,412 textual descriptions from 13,003 identities. The training set includes 34,504 images, 11,003 identities, and 68,126 textual descriptions. The validation set consists of 3,078 images, 1,000 identities, and 6,158 textual descriptions. The test set includes 3,074 images, 1,000 identities, and 6,156 textual descriptions.

**Table A: Performance of various pre-trained models on CUHK-PEDES [25]. Fine-Tune denotes the CLIP model fine-tuned according to the settings in this paper.**

No.	Backbone	Method	Rank-1	Rank-5	Rank-10	mAP
1	ViT-B/16	CLIP	12.606	27.112	35.559	11.145
2		Fine-tuned	<b>73.847</b>	<b>89.571</b>	<b>93.681</b>	<b>68.086</b>
3	ViT-L/14	CLIP	10.185	23.262	30.962	9.192
4		Fine-tuned	<b>75.991</b>	<b>90.578</b>	<b>94.428</b>	<b>68.337</b>

**Table B: Impact of different forms of loss functions**

No.	Method	Loss	Rank-1	Rank-5	Rank-10	mAP
1	$\mathcal{L}_{Vis}$	ITC	35.786	57.221	65.168	45.848
2		CMPM	<b>38.919</b>	<b>59.310</b>	<b>67.075</b>	<b>48.538</b>
3	$\mathcal{L}_{Text}$	ITC	36.648	60.082	68.256	47.455
4		CMPM	<b>40.054</b>	<b>61.262</b>	<b>68.574</b>	<b>49.903</b>

ICFG-PEDES [8] includes 54,522 textual descriptions corresponding to 54,522 images of 4,102 identities. Each image is associated with a single textual description, and the vocabulary consists of 5,554 unique words. The dataset is split into training and test sets with 34,674 image-text pairs of 3,102 identities, and 19,848 image-text pairs of the remaining 1,000 identities, respectively.

RSTPReid [57] contains 20,505 images from 4,101 different identities, captured by 15 cameras. Each identity has 5 images taken from different cameras, and each image is accompanied by a textual description containing no fewer than 23 words. For dataset partitioning, the training, validation, and test sets are composed of 3,701, 200, and 200 identities, respectively.

## C ADDITIONAL RESULTS

### C.1 Fine-tuning Results

In the fine-tuning process of Word4Per, the objective is to make the model capable of performing TPR task effectively. In line with this, we also evaluate the performance of the fine-tuned models on the CUHK-PEDES test set, and the results are shown in Table A. It can be observed that fine-tuning the parameters of CLIP [37] is essential.

### C.2 Effectiveness of the Loss Function.

A comparison is made between the CMPM [20] loss and the Image-Text Contrastive (ITC) [38, 46] loss, which is commonly used in the CIR task. The results, as shown in Table B, demonstrate that superior performance is consistently achieved by employing the CMPM loss with supervised optimization method. This also indicates that, for the CPR task, it is not appropriate to treat each image-text pair as an individual category but rather to consider all image-text pairs of the same identity as a single category, as they share all characteristics, including attire.

### C.3 Word4Per with Smaller Data Volumes.

We conduct training of the TINet by extracting original data at different proportions to observe if utilizing more data will yield

better results. As shown in Table C, the experimental results show that even when using a randomly initialized TINet, it does not result in significant performance loss (No. 1 and No. 2). With a small amount of data available for training (No. 3 and No. 9), Word4Per performance still surpasses all previous methods. Furthermore, the results of experiments No. 9-14 lead to the following conclusions: when optimizing the TINet under  $\mathcal{L}_{Text}$  supervision on the same dataset, training with more image-text pairs can result in superior performance. For  $\mathcal{L}_{Vis}$  supervised optimization (No. 3-7), this trend is similar to  $\mathcal{L}_{Text}$ , while No. 8 exhibits marginally superior performance compared to No. 7 due to the impact of low-quality images and noise in the dataset.

### C.4 Fusion Retrieval

Depending on the flexibility of Word4Per, during testing, the simultaneous utilization of multiple TINets for fusion retrieval is possible. The performance of the related methods on the ITCPR dataset is shown in Table 1 (No. 8-10 and No. 22-24), in which TINet adopts the optimal structure (Sec. 5.3). In contrast, employing an appropriate fusion strategy often leads to the best performance and has a broader range of choices.

### C.5 Balancing Efficiency and Precision

In this section, we delve into how to achieve optimal performance based on the current framework, as well as the corresponding retrieval efficiency for different approaches. The relevant results are presented in Table D. By using the optimal text inversion network under the supervision of  $\mathcal{L}_{Vis}$  and training the extended data, experimental results No. 2-3 and No. 9-10 are obtained. This represents the optimal performance achievable with a single textual inversion network. A substantial improvement is achieved when employing two textual inversion networks for fusion (No. 4-6 and No. 11-13). Among them, the TINets using the same supervision optimization have the smallest fusion improvement (No. 6 and No. 13), even if their single network performance is outstanding. Further gains in performance are achieved when using three textual inversion networks, albeit to a lesser extent (No. 7 and No. 14). It can thus be inferred that fusing more well-trained textual inversion networks leads to better performance, though the degree of improvement diminishes. Moreover, examining the variations in inference time in the table indicates that using more textual inversion networks is accompanied by a reduction in retrieval efficiency. When applying this method, it is crucial to flexibly select a fusion scheme based on the specific practical application scenario.



**Table C: Impact of extracting data at different proportions from the same dataset for training. “Random” indicates the usage of randomly initialized TINet.**

No.	Method	Rank-1	Rank-5	Rank-10	mAP	Dataset	No.	Method	Rank-1	Rank-5	Rank-10	mAP
1	Random	25.749	45.822	55.767	35.581	-	2	Text-only	26.385	46.458	56.267	36.132
3	$\mathcal{L}_{Vis}$	32.334	50.727	58.629	41.261	10%	9	$\mathcal{L}_{Text}$	32.970	51.680	59.310	41.727
4		33.106	54.269	62.807	43.192	20%	10		34.242	55.040	63.259	43.744
5		34.514	54.541	64.850	44.760	30%	11		35.195	55.632	64.124	44.650
6		36.376	57.902	66.213	46.679	50%	12		37.125	57.026	65.468	46.951
7		38.374	<b>59.855</b>	<b>67.757</b>	<b>48.502</b>	75%	13		38.583	59.819	67.813	48.631
8		<b>38.919</b>	<u>59.310</u>	<u>67.075</u>	<b>48.538</b>	100%	14		<b>40.054</b>	<b>61.262</b>	<b>68.574</b>	<b>49.903</b>

**Table D: Performance under different strategies. The symbol & in the method denotes fusion testing using the TINets of corresponding experiments.  $IPR$  represents the image dataset as described in Section B.2, and  $IPR^{10\%+}$  involves selecting the highest 10% resolution images to form a new dataset, mitigating the impact of low-quality images. The time in the table represents the duration required for the respective method to complete all retrieval tasks on the entire ITCPR dataset, thus avoiding potential statistical anomalies.**

No.	Backbone	Dataset	Method	Time (s)	Rank-1	Rank-5	Rank-10	mAP
1	ViT-B/16	$C$	$\mathcal{L}_{Text}$	30.656	40.054	61.262	68.574	49.903
2		$C+I+R$	$\mathcal{L}_{Vis}$	30.454	41.826	62.307	69.391	51.353
3		$IPR^{10\%+}$	$\mathcal{L}_{Vis}$	30.453	41.508	62.080	69.028	50.825
4		-	$No.1\&2$	31.020	<u>43.415</u>	63.442	70.663	<u>52.740</u>
5		-	$No.1\&3$	31.081	<u>43.415</u>	<u>63.488</u>	<u>70.754</u>	52.622
6		-	$No.2\&3$	30.997	42.461	63.124	70.481	52.073
7		-	$No.1\&2\&3$	31.574	<b>43.551</b>	<b>63.760</b>	<b>71.026</b>	<b>53.041</b>
8	ViT-L/14	$C$	$\mathcal{L}_{Text}$	65.130	45.549	66.803	74.796	55.260
9		$C+I+R$	$\mathcal{L}_{Vis}$	64.986	45.595	65.168	72.616	54.755
10		$IPR^{10\%+}$	$\mathcal{L}_{Vis}$	64.979	45.549	66.167	73.025	54.906
11		-	$No.8\&9$	66.063	<u>47.184</u>	68.256	<u>75.023</u>	<u>56.790</u>
12		-	$No.8\&10$	66.069	47.048	<u>68.483</u>	74.796	56.636
13		-	$No.9\&10$	65.913	46.458	66.803	74.069	55.688
14		-	$No.8\&9\&10$	66.475	<b>47.502</b>	<b>68.392</b>	<b>75.103</b>	<b>56.944</b>